Maulana *et al. Geoscience Letters* (2023) 10:40
https://doi.org/10.1186/s40562-023-00293-8

Geoscience Letters

RESEARCH LETTER

Open Access

Regional variation of the influence of cross-equatorial northerly surge towards diurnal cycle of rainfall over Java Island

Madam Taqiyya Maulana[1*], Takeshi Yamazaki[1], Toshiki Iwasaki[1] and Muhammad Rais Abdillah[2]

Abstract

Cross-equatorial northerly surge (CENS) is known to cause torrential rainfall over Java Island in the Maritime Continent. Some studies indicated that the rainfall increase is attributed to changes in the diurnal cycle of rainfall (DCR) in northwestern Java. It is not well understood whether the DCR changes are present in the other parts of Java Island and whether the changes are similar to those in northwestern Java. This study performs climatological analyses to investigate the regional variation of the influence of the CENS on the DCR over Java Island using IMERG and ERA5 data sets of 20 years of boreal winter. We find that there are differences in intensity, timing, and coverage of DCR responses over western, central, and eastern Java. CENS modifies the timing of coastal rainfall on the northern coast, resulting in early morning rainfall enhancement owing to the convergence between the incoming northerlies and land breeze. A small increase in early morning rainfall is observed in eastern Java, possibly due to the northerly flow gaining more zonal components on the eastern coast, which then results in relatively weaker convergence than the western coast. The timing of early morning rainfall appears to be slightly different between the three areas. CENS is also found to suppress afternoon rainfall inland because of increasing static stability due to cold air advection from the north. The suppression varies from western to eastern Java, with the largest suppression seen in western Java. Relatively narrower and wider suppression areas are found in central and eastern Java, respectively. These differences are attributed to the topography characteristics of Java.

Keywords Diurnal cycle of rainfall, Cross-equatorial northerly surge, IMERG, Java Island

Introduction

Cross-equatorial northerly surge (CENS) events are known to enhance the rainfall over Java Island in the Maritime Continent (MC; Wu et al. 2007; Hattori et al. 2011; Trilaksono et al. 2012; Mori et al. 2018; Yulihastin et al. 2020; Hermawan et al. 2022). CENS is characterized by low-level strong northerly winds higher than 5 m s^{-1} within 105°E–115°E and 5°S–EQ that occurs intermittently during boreal winter (Hattori et al. 2011). The strong East Asian monsoon flow in boreal winter could promote the CENS event through cold surge events or directly strengthen the northerly flow below the equator. Abdillah et al. (2021) showed that strong midlatitude cold surges passing the South China Sea (SCS) and the Philippines Sea significantly trigger the development of northerlies south of the equator.

The diurnal cycle of rainfall (DCR) is the pronounced rainfall characteristic over the MC. The prominent pattern of the DCR is the presence of a rainfall peak, called the DCR phase. The diurnal convection pattern in the MC basically is driven by diurnally developed

*Correspondence:
Madam Taqiyya Maulana
madamtaqiyya@gmail.com
[1] Department of Geophysics, Graduate School of Science, Tohoku University, 6-3 Aza-Aoba, Aramaki, Aoba-Ku, Sendai, Miyagi 980-5878, Japan
[2] Atmospheric Science Research Group, Faculty of Earth Sciences and Technology, Bandung Institute of Technology, Bandung 40132, Indonesia

circulation, generated by the thermal contrast between land and sea, such as sea-land or mountain–valley breeze interaction (Houze et al. 1981). This circulation results in the particularity of the DCR pattern over the land and the sea. For example, the land is predominated by the afternoon to evening phase, while the offshore is predominated by the morning phase (Mori et al. 2004; Qian 2008; Wu et al. 2009; Qian et al. 2010). Or in another way, the thermal contrast between land and sea could be a result of the DCR itself (see Yamanaka et al. 2018).

Since the rainfall characteristic in the MC is predominated by a diurnal pattern, the influence of CENS on the DCR becomes important. There have been several studies concerning the influence of CENS on the DCR. Yulihastin et al. (2020) suggested that the early morning rainfall peak over northwestern Java in the boreal winter is mainly caused by CENS. The early morning increase also appears in the recent study on the SCS cold surge by Krismon et al. (2022). This change in DCR was linked to several extreme events, such as heavy rainfall and flood events in the Jakarta region (northwestern Java), where the timing of heavy rainfall was observed in the early morning to morning (Wu et al. 2007; Trilaksono et al. 2012; Saufina et al. 2021). Besides the early morning rainfall peak, a study by Mori et al. (2018) using a 1-month radar observation also showed afternoon rainfall suppression in Bogor (northwestern Java) during CENS.

The influence of CENS was also observed in Semarang City (central Java) (Hermawan et al. 2022). However, the rainfall initiation location in central Java during CENS is quite different from northwestern Java. The nighttime rainfall initiation was observed in the coastal land in Semarang city of central Java during the CENS event and led the heavy rainfall in the early morning. Meanwhile, the early morning rainfall over northwestern Java during CENS comes from offshore (Yulihastin et al. 2020, 2022). The difference in rainfall initiation indicates that the DCR in each region might respond differently to CENS.

Though some changes in the DCR during CENS have been revealed in previous studies, there has been no climatological investigation on the regionality of the influence of the CENS on the DCR between western Java, central Java, and eastern Java. Furthermore, the mechanism of how the DCR responds differently in Java Island is not well understood. Hence, this study aims to systematically investigate the regional variation of influence of CENS on the DCR over Java Island in the recent 20 years and discuss possible mechanisms that may play roles in the DCR changes.

Data and methods

To study the DCR over Java Island, a high spatiotemporal resolution of climate data is required to cover the diurnal time scale and the complex topography of Java Island. Hence, this study used one of the Global Precipitation Measurement (GPM) products, namely, the integrated multi-satellite retrievals for GPM (IMERG) Final Run version 06 (Huffman et al. 2019) with a relatively high spatial and temporal resolution of 0.1° and half-hourly, respectively. GPM is the successor to TRMM initiated by the National Aeronautics and Space Administration (NASA) and the Japan Aerospace Exploration Agency (JAXA; Hou et al. 2014). In our preliminary analyses, IMERG shows better homogeneity over the coastal area than the Global Satellite Mapping of Precipitation reanalysis (GSMaP) Version 7 (see Additional file 1). Recent studies also show that IMERG could provide good observation and depict the DCR over the MC (Tan et al. 2019; Andi et al. 2020; Ramadhan et al. 2022a, 2022b).

We also use the fifth-generation of European Centre for Medium-Range Weather Forecast (ECMWF) atmospheric reanalysis of the global climate (ERA5; Hersbach et al. 2020) data set to obtain other supporting variables for the analysis. It has 0.25° spatial resolution and hourly temporal resolution. Our preliminary analysis of the CENS impact on the daily rainfall shows that the ERA5 daily rainfall anomalies are similar to IMERG daily rainfall anomalies during CENS (see Additional file 1).

The climatological analysis is conducted from December–February 2000/2001 to December–February 2019/2020. To determine CENS day, firstly we define a CENS index by averaging daily 10-m meridional wind over 105°E–110°E, 5°S–EQ (see Fig. 1). The index is then multiplied by −1, so that the northerlies are indicated by positive values. CENS days are identified when the anomalies of CENS index exceed one standard deviation. Note that the current CENS definition is slightly different from the definition in Hattori et al. (2011). Hattori's et al. (2011) utilize sea surface wind over a wider area that extends eastward covering a large part of Borneo (see Fig. 1 of Hattori et al. 2011), thus the method is less convenient since it requires removal of grid points overlapped with land to obtain sea surface wind. The area for the new index is narrower and almost entirely located over the sea. The new index also focuses on the western part of Hattori's et al. domain that is closer to the SCS, where cold surge comes from. In addition, we use a climatological mean-based threshold rather than a fixed-value threshold to define CENS. This approach enables future inter-comparison analysis of climate models. Through this procedure, 294 CENS days and 1,511 non-CENS days are identified during the study period. Some recent studies discussing CENS also develop their own

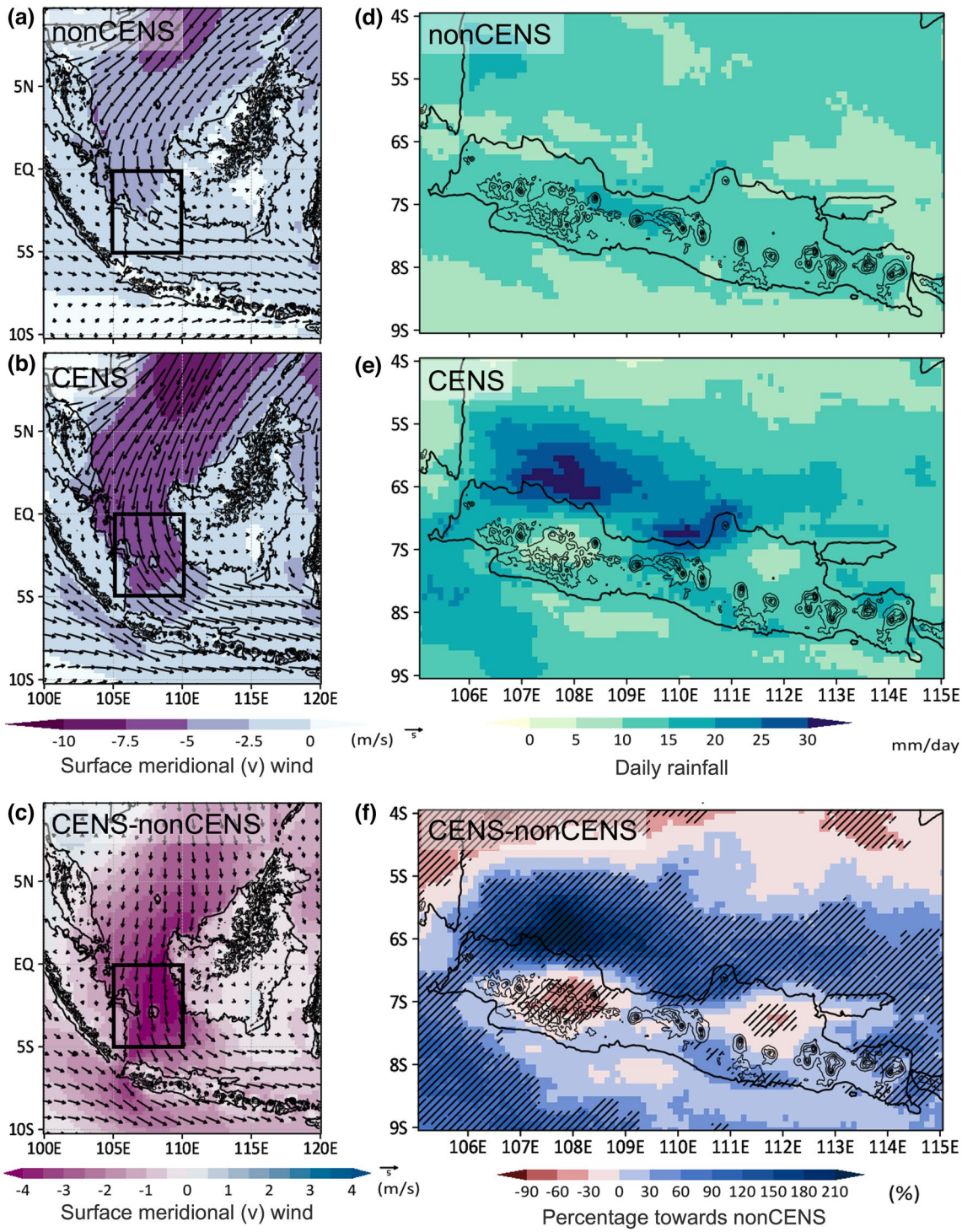

Fig. 1 **a–c** ERA5 daily mean of surface wind [vector;ms^{-1}] overlayed with the meridional wind [shaded; ms^{-1}] and **d–f** daily mean of rainfall [shaded; mm day^{-1}] of IMERG for **a, d** nonCENS, **b, e** CENS, **c** surface wind difference between CENS and nonCENS (CENS–nonCENS) and **f** daily rainfall of $\frac{\text{CENS}-\text{nonCENS}}{\text{nonCENS}} \times 100\%$[The positive (negative) value in the blue (red) is the enhancement (reduction) percentage of daily rainfall during CENS to nonCENS]. The hatched areas indicate the rainfall difference during CENS and nonCENS satisfies 95% confidence levels of the statistical significance test. The black rectangle indicates the used CENS index area in this study

index according to their interests. Such as Xavier et al. (2020) and Yulihastin et al. (2022). We still could see that with our method, CENS days are characterized by strong northerly winds above 5 ms^{-1} over the sea, coherent with the definition by Hattori et al. (2011).

We divide Java Island into western Java (WJ), central Java (CJ), and eastern Java (EJ) to study the regionality of the influence of CENS. We also investigate the change in the DCR phase by CENS. The DCR phase is obtained by finding the peak of the rainfall from the composite of CENS and nonCENS days.

Results and discussion

In boreal winter, the northeasterly mean wind blows over the SCS and turns northwesterly after crossing the equator, bringing rich moisture from the northwestern equatorial Pacific into the southern MC. The northerly components of the wind during nonCENS and CENS are shown in Fig. 1. Northerly wind higher than 5 m s^{-1} is located far north of the equator during nonCENS, while it extends to the south of the equator during CENS. The difference shown in Fig. 1c denotes the strengthening of northerly wind from the SCS to the south of Java Island.

Different surface wind condition results in different daily rainfall patterns. During nonCENS, the heavy rainfall tends to be in the center of the Island, while notably high daily rainfall areas are observed on the northern coast and small areas on the southern coast of EJ during CENS. The daily rainfall during CENS is enhanced by more than 200% of the total daily rainfall during nonCENS in northwestern Java. Moreover, Fig. 1f clearly shows that CENS also suppresses the daily rainfall over inland areas up to 30–60% of the total daily rainfall during nonCENS, especially over WJ and EJ. Overall, the daily wind and rainfall changes during CENS presented here are consistent with previous studies (e.g., Hattori et al. 2011). However, previous studies put less emphasis on the pattern of rainfall reduction inland.

DCR phase shifting

The early morning rainfall enhancement over the coastal sea and the afternoon rainfall suppression inland caused the change of the DCR phase on Java Island during CENS. Figure 2a shows most of the coastal area of Java Island is predominated by the afternoon–evening phase, 12–23 local time (LT), during nonCENS, except for the coastal sea in northern WJ which is predominated by the midnight–early morning phase, 00–06 LT, similar to the DCR phase over the adjacent sea that surrounds Java Island. CENS shifts the DCR phase in the coastal area from the afternoon–evening phase to the midnight–early morning phase, especially in WJ, where the midnight–early morning phase emerges further inland up to the foothill of the mountainous region (Fig. 2b).

The time difference between the DCR phase during CENS and nonCENS varies regionally (Fig. 2c). Over most mountainous areas the time differences are quite small compared with the coastal and offshore areas. In the coastal land of north WJ and EJ, the time difference is 6–12 h, where the rainfall peak during CENS is later (blue-shaded) than during nonCENS. In the coastal sea and offshore, the rainfall peak during CENS is earlier (red-shaded) than during nonCENS.

The change in the diurnal pattern for some areas is visible in Fig. 2d. In the offshore (OS), the phase is shifted from late morning peak (07–10 LT) to midnight–early morning (00–06 LT). In the coastal sea (CS), the early morning (01–04 LT) is shifted to midnight. OS and CS phase remains in the land breeze regime. In the mountainous area (MT), the phase remains in the sea breeze regimes, around 16 LT in both nonCENS and CENS. However, in the coastal land (CL), the phase is shifted from late afternoon (16 LT) to early morning (01 LT), where the dominant wind is sea breeze in the later afternoon and land breeze in the early morning. In Fig. 2c, the dark blue color significantly indicates the switching of rainfall peaks from late afternoon to early morning.

Early morning rainfall enhancement by CENS on the northern Java coast

Figure 3 shows the hovmöller diagram of the meridional variation of the DCR for WJ, CJ, and EJ during nonCENS, CENS, and the difference between CENS and nonCENS based on the subset area shown in Fig. 4. The pronounced impact of CENS in the three regions is the enhancement of early morning rainfall in the northern coastal area. However, the intensity of the enhancement is different between the three regions. The largest early morning rainfall enhancement is observed in WJ and the lowest is in EJ. The intensity of early morning rainfall enhancement seems to be proportional to the strength of the northerly wind in each region.

The three regions also show differences in the rainfall propagation and the timing of the peak of the early morning rainfall during CENS. The peak of the early morning rainfall in northern WJ is earlier (before 03 LT) than in northern CJ and EJ (after 03 LT). The timing of the early morning peak in WJ and CJ in this study is similar to the several case studies of extreme rainfall in Jakarta (WJ) and Semarang (CJ; Trilaksono et al. 2012; Saufina et al. 2021; Hermawan et al. 2022). The heavy rainfall in the nighttime is initiated earlier offshore for WJ with more evident southward propagation, while it occurs in the coastal land and later (late evening) for northern CJ and EJ with weak northward propagation. As for north CJ,

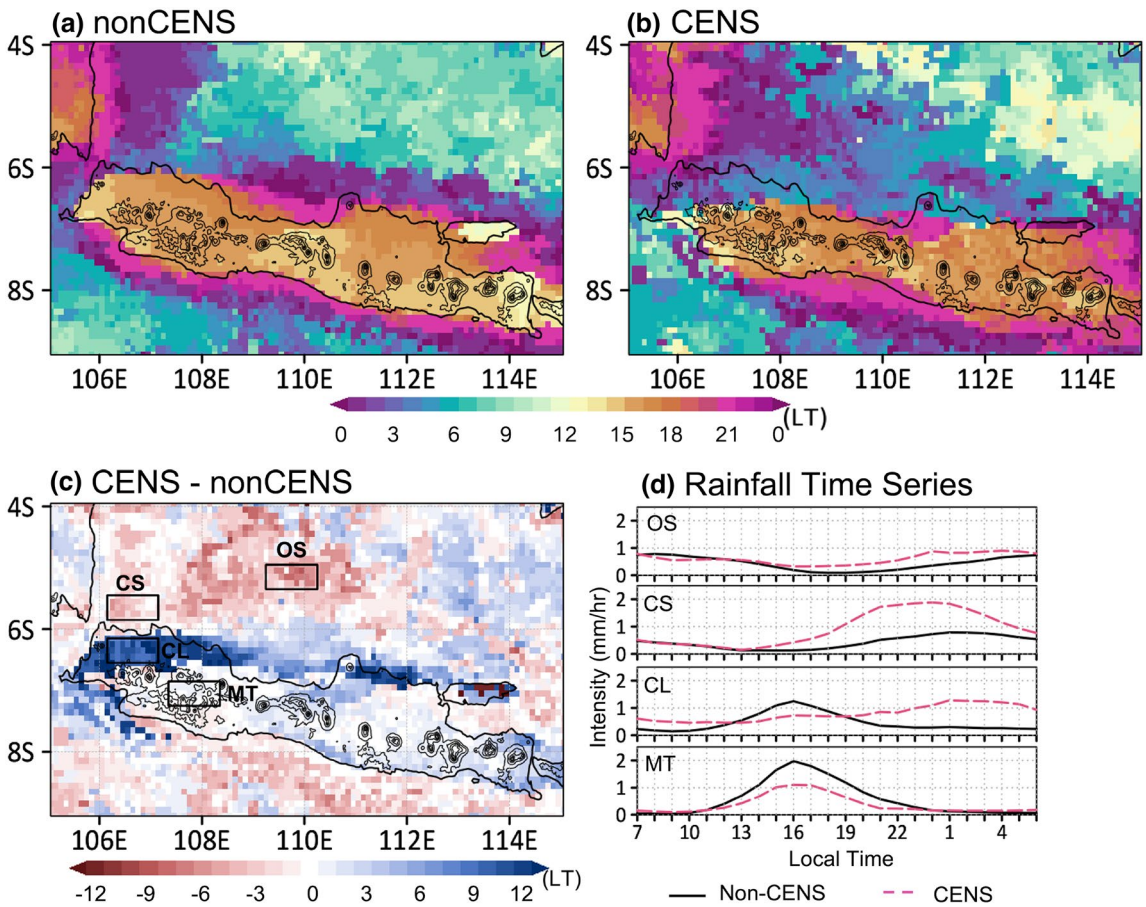

Fig. 2 Spatial pattern of the DCR phase [shaded; local time] during **a** nonCENS, **b** CENS, and **c** the time difference between CENS and nonCENS phases. The negative value [red-shaded] means the DCR phase during CENS is earlier, and the positive value [blue-shaded] means the DCR phase during CENS is later. Panel **d** is the time series of the diurnal rainfall that represents the offshore area (OS), coastal sea area (CS), coastal land area (CL), and mountainous area (MT) [solid black lines are for nonCENS; dashed pink lines are for CENS]

there are two peak times that appear in the coastal area. The first peak is in the evening and the second peak time is in the early morning. The double peak structure during CENS over CJ also appears in a study case of heavy rainfall on February 6, 2021, in Semarang by Hermawan et al. (2022).

The differences in the nighttime rainfall propagation direction and the timing of the early morning rainfall are likely to be determined by the location of the rainfall initiation. Figure 5 shows three hourly evolutions of rainfall and the overlayed vertically integrated moisture flux convergence (VIMFC) with surface wind convergence and the diurnal component of surface wind. During nonCENS and CENS, nighttime rainfall is observed in the coastal sea in north WJ that comes from southeastern Sumatra Island with different characteristics. The rainfall in southeastern Sumatra appears to start in the late afternoon, 16 LT, during nonCENS and CENS. However, the rainfall location is shifted southward under the influence of CENS with a smaller rainfall coverage area, since the afternoon rainfall in Sumatra Island is also greatly reduced. The afternoon rainfall from southeastern Sumatra propagates eastward towards the Java Sea during nonCENS, thus the rainfall remains offshore with light rainfall observed on the northern coast at WJ in the nighttime. Meanwhile, during CENS, the rainfall is greatly intensified when it reaches the coastal sea in the nighttime and propagates eastward and southward simultaneously towards Java Island. Strong VIMFC in the coastal sea of north WJ allows the rainfall to intensify significantly when it reaches the sea. The large coverage area of the rainfall from southeastern Sumatra intrudes the north WJ further inland as it propagates southward, which is also supported by the stronger surface wind convergence near the coastal area, in the late evening to the early morning (23–05 LT). This condition could allow the convective system to become a bigger system, like the mesoscale convective system (MCS), as observed in

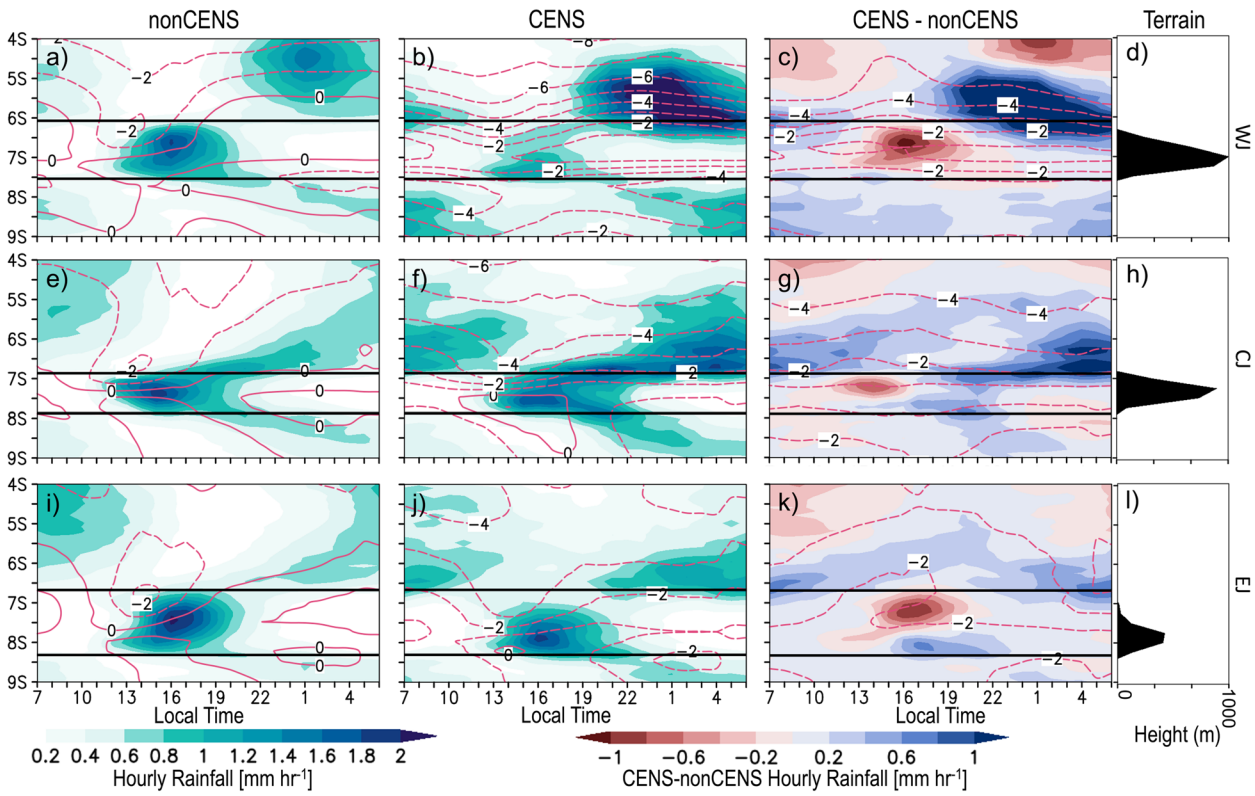

Fig. 3 Hovmöller diagram of the hourly rainfall [shaded; mm h^{-1}] and the meridional component of surface wind during [solid contour for southerly; dashed contour for northerly; m s^{-1}) for **a, e, i** nonCENS, **b, f, j** CENS, and **c, g, k** the difference between CENS and nonCENS for **a–c** WJ region, **e–g** CJ region, and **i–k** EJ region. The topography feature of WJ, CJ, and EJ are shown in panels (**d, h, and l**), respectively

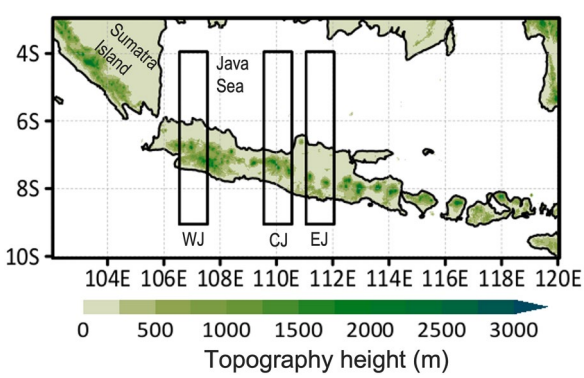

Fig. 4 Topography of Java Island [shaded; meter] and subset area of western Java (WJ), central Java (CJ), and eastern Java (EJ)

a study case of heavy rainfall event during CENS in 2013 over the Jakarta region (WJ) by Nuryanto et al. (2019).

In north CJ, rainfall in the coastal area already occurs in the late afternoon (around 16 LT) and later propagates to the sea (northward) in the nighttime during nonCENS and CENS. During nonCENS, the rainfall in the coastal land has already vanished around 22 LT as it propagates further to the sea. However, seaward propagation is hindered by the CENS. During CENS, the rainfall is still on the coastal land at 22 LT and stays in the coastal area until the morning. The rainfall is enhanced, while it stays in the coastal area, where the surface wind convergence is intensified throughout the land breeze regime. In addition, it is possible that the rainfall system from southeastern Sumatra propagates further eastward and merges with the rainfall system in north CJ as identified in the numerical study by Yulihastin et al. (2022). Though the surface wind convergence is stronger in north CJ, the nighttime rainfall is more intense in north WJ than in north CJ due to stronger VIMFC and wider coverage of VIMFC in north WJ than in north CJ. Since the strength of VIMFC significantly affects the intensity of the early morning rainfall, we could expect a similar mechanism and rainfall propagation direction in EJ, where the wind is gaining more zonal components resulting in weaker VIMFC.

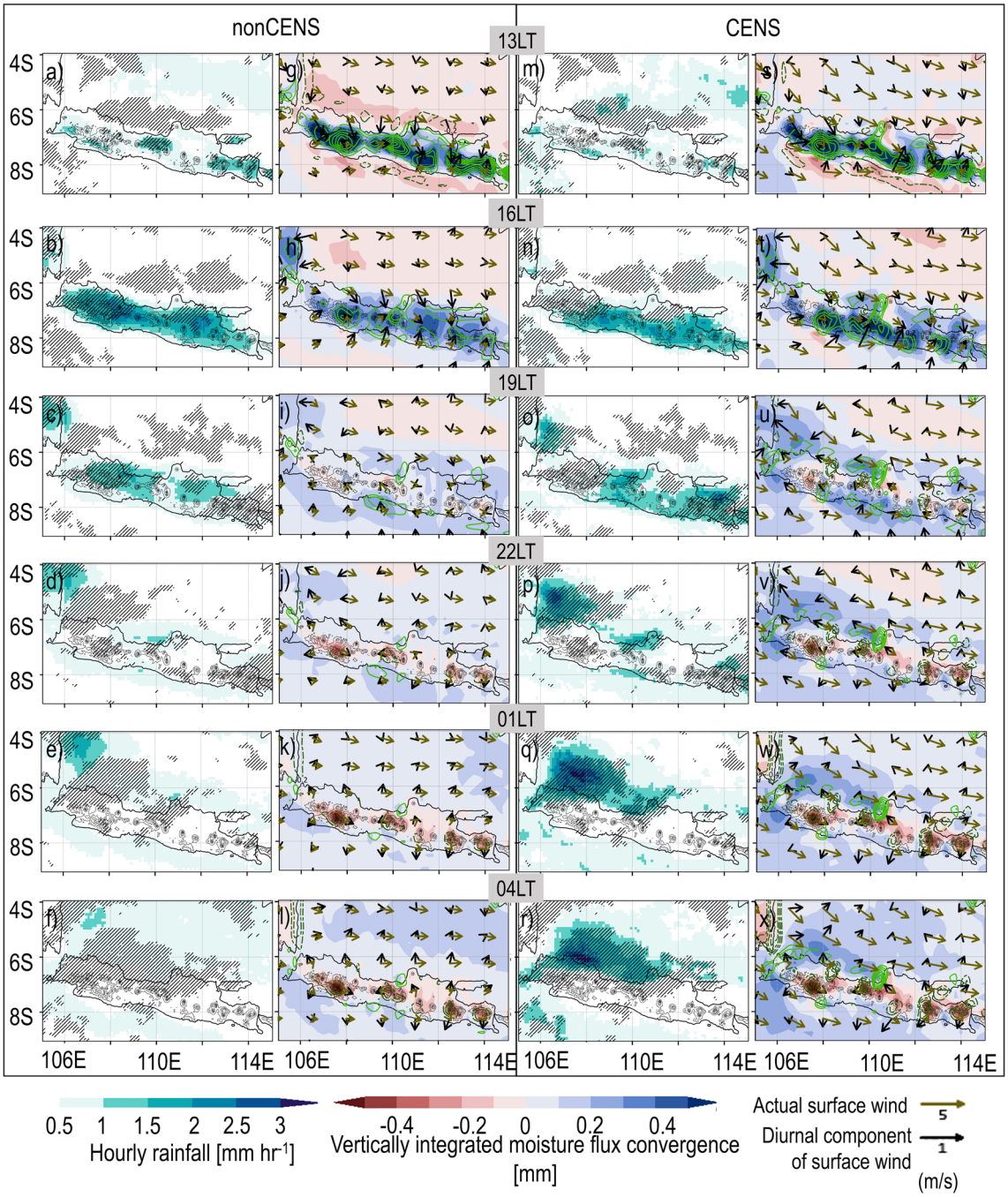

Fig. 5 Hourly evolution of **a–f, m–r** rainfall [shaded; mm h^{-1}] and **g–l, s–x** overlayed vertically integrated moisture flux convergence (VIMFC) from 1000 to 850 hPa (shaded; mm) with surface wind convergence [red contour; s^{-1}] and surface wind [vector; m s^{-1}] from 13 to 04 LT with 3 h interval during nonCENS and CENS, respectively. The solid green contour is convergence and the dashed dark green contour is divergence. The brown arrow indicates the actual wind, while the black arrow indicates the diurnal component of the surface wind. The hatched areas indicate the rainfall difference during CENS and nonCENS satisfies 95% confidence levels of the statistical significance test

Afternoon rainfall suppression by CENS over the inland area

Another pronounced impact of CENS could be seen in the afternoon rainfall inland (Fig. 3). The afternoon rainfall is initiated from the high terrain in WJ, CJ, and EJ during nonCENS. In WJ and EJ, the afternoon rainfall is initiated from the south, while the afternoon rainfall is initiated from the north in CJ. However, the rainfall

initiation is shifted to the south during CENS in the three regions. Moreover, the afternoon rainfall inland is suppressed significantly in WJ with a large coverage area, followed by EJ, then CJ. In CJ and EJ, the suppression occurs in the north, followed by rainfall enhancement in the south. Although the northerly wind is stronger in CJ than in EJ, the afternoon rainfall suppression in EJ is greater and covers a wider area than in CJ.

As shown in Fig. 5, the rainfall pattern in the afternoon seems to coincide with the surface wind convergence which is more concentrated in the southern part during CENS. The strong VIMFC in the afternoon slightly shifted to the south during CENS compared to nonCENS. Nevertheless, the value and the pattern of VIMFC and surface wind convergence are not greatly reduced, while the afternoon rainfall intensity is significantly reduced and dispersed quickly.

Figure 6 shows the vertical cross-section of daytime averages (10–16 LT) of the virtual potential temperature (θ_v) and the actual meridional circulation for the three regions during nonCENS, CENS, and the difference between CENS and nonCENS. The three regions show differences in the topographical feature. WJ and EJ have wider land widths compared with CJ. The high terrain or mountainous region in WJ predominates from the southern part to the central. In CJ, the high terrain is closer to the northern coast. In EJ, the high terrain tends to be in the south.

The northerly wind and southerly wind in the daytime converge inland in the three regions during nonCENS (Fig. 6a, d, and g). The area of convergence is indicated by the perpendicular arrows shown over the high terrain in WJ and CJ and most inland areas in EJ. During CENS, the strong northerly wind predominates inland in the daytime, especially in WJ, and weakens the convergence on the northern side. While in CJ, the southerly wind is still observed in the southern part. The strong northerly wind shifts the convergence area to the south in CJ and EJ.

Figure 6c, f shows that the wind difference between CENS minus nonCENS yields upward directions on the windward side. This condition is the result of the interaction between the strong northerly wind and the high terrain. The strengthening of northerly wind during CENS reinforces air parcels to climb up the high terrain in WJ and CJ and results in stronger upward motions. In EJ, the northerly wind is weaker and the terrain is lower than WJ and CJ located in the southern part of EJ, thus the downward motion is visible in the northern low plain area (Fig. 6i) that might help to suppress the convective activity in that area.

Figure 6c, f, and i shows that the lower θ_v resides on the northern side of the mountainous and slightly higher θ_v area on the southern side during CENS. Lower θ_v during CENS might reduce the buoyancy of the air parcel and form a more stable layer. The latest study by Satiadi et al. (2023) supports this argument showing that the convective available potential energy (CAPE) is reduced during CENS. In WJ, the lower θ_v intrudes further to the southern part of the mountainous region, covering most of the inland area. In EJ, the inland intrusion of lower θ_v is further to the south than CJ. The lower topography

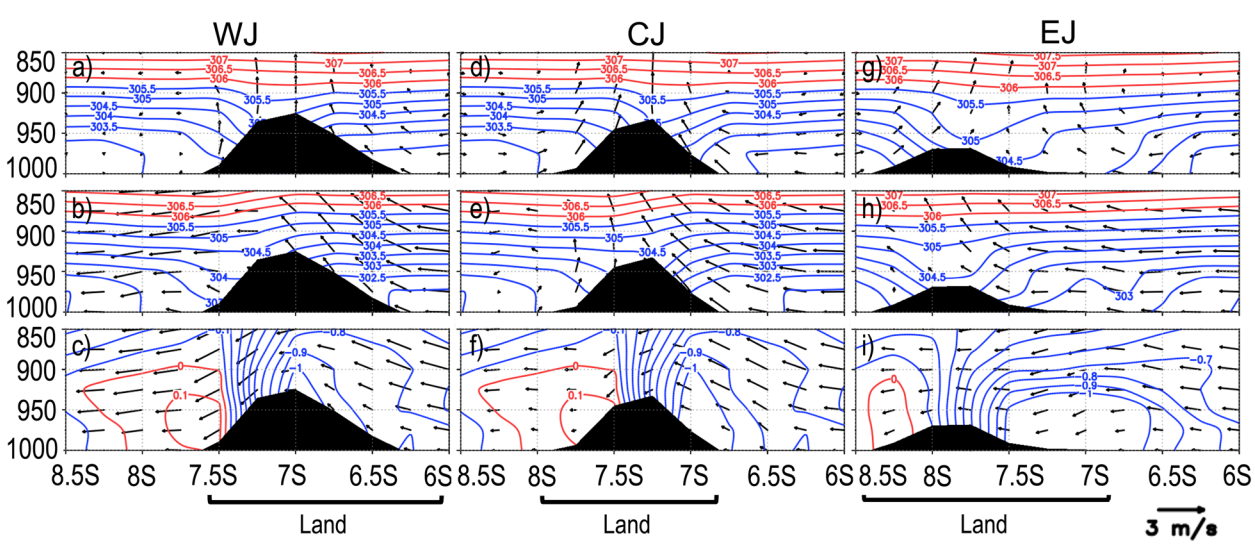

Fig. 6 Vertical cross section of daytime (10–16 LT) composite of virtual potential temperature (θ_v) from ERA5 [contour; K] and meridional circulation [actual v-wind and w-wind (multiplied by 10); vector; m s^{-1}] over **a–c** WJ, **d–f** CJ, and **g–i** EJ for **a, d, g** nonCENS, **b, e, h** CENS and **c, f, i** difference between CENS and nonCENS (CENS - nonCENS)

barrier or lower and less complex mountainous area in EJ allows the lower θ_v to intrude further to the south and hence suppress the afternoon rainfall, though the northerly wind in EJ is weaker than in CJ. In conclusion, possible factors that influence the afternoon rainfall during CENS are not only the moisture flux and wind convergence. During CENS, the lower θ_v assists the suppression of the afternoon inland rainfall over Java Island.

Koseki et al. (2013) also showed a similar vertical profile of θ_v in their model experiment on a cold tongue event that governs strong northerly wind over Java Island. They suggested that the lower θ_v in the afternoon is related to the colder land surface temperature due to higher surface latent heat inland caused by the strong northerly wind. In other words, the strong northerly wind conduces land surface cooling that generates the stable layer. However, surface latent heat flux released by the strong wind is more significant over the sea. As it is shown in our analysis of surface latent heat flux (see Additional file 2) shows that the daytime surface latent heat flux inland is lower during CENS than nonCENS, and higher over the sea. Moreover, the lower air temperature and higher relative humidity in the daytime during CENS reside in the northern part of Java Island, where the lower θ_v exists and afternoon rainfall is suppressed which makes it difficult to release greater latent heat flux. Thus, we suggest that the stable layer in the afternoon which suppresses the afternoon rainfall over the land is associated with the cold air which is advected by CENS to the northern part of Java Island.

Conclusion

The daily rainfall over the inland and coastal areas shows different responses to CENS events. The inland rainfall is suppressed, and the northern coast rainfall is increased. Both responses are attributed to specific changes in the diurnal cycle. The former is related to the decrease in afternoon rainfall and the latter is to the increase in early morning rainfall. These overall features commonly appear in WJ, CJ, and EJ. However, they show different regional characteristics in the intensities, timing, and area coverage of the DCR. The regional differences for each WJ, CJ, and EJ in response to CENS events are summarized in Table 1.

The CENS modifies the timing of coastal rainfall in the north, resulting in early morning rainfall enhancement owing to the convergence between the incoming northerlies and land breeze. This pattern is observed over the whole northern coast. The small increase in early morning rainfall is observed in EJ, possibly due to the northerly flow gaining more zonal components on the eastern coast, which then results in relatively weaker convergence than the western coast. The initiation location and timing of early morning rainfall appear to be slightly different between the three areas. In WJ, the early morning rainfall with the southward direction intrudes further into the mountain foothills. In CJ and EJ, the early morning rainfall with the northward direction stays in the coastal area. The timing of early morning rainfall in WJ is earlier (before 03 LT) compared to CJ and EJ (after 03 LT).

The CENS is also found to suppress afternoon rainfall inland because of the strengthening of horizontal wind and increasing static stability due to cold air advection from the north. The suppression varies from WJ to EJ, with the largest suppression seen in WJ. Relatively narrower and wider suppression areas are found in CJ and EJ, respectively. These differences are attributed to the topography characteristics of Java. Even though the northerly wind is weaker in EJ, the location of the mountainous area is far to the south, thus the lower θ_v which assists in suppressed afternoon rainfall could penetrate further to the south in EJ than in CJ.

This study focuses on the general characteristics of CENS and nonCENS days. However, the signatures shown here may be sensitive to any possible interactions with other phenomena, such as the Madden–Julian Oscillation (MJO). We count that CENS/nonCENS days are associated with different MJO phases (see Additional file 3) and thus CENS occurring in different phases of MJO may yield different impacts. This possible dependency is important to be investigated in the future. A recent study by Satiadi et al. (2023) gives some insights as they revealed the difference in diurnal rainfall response to CENS during different phases of MJO.

Table 1 Regional differences in response to CENS events

	Afternoon rainfall suppression			Early Morning Rainfall Enhancement		
	Intensities	**Coverage**	**Timing**	**Intensities**	**Coverage**	**Timing**
WJ	Large reduction	Most Inland area	13–20 LT	Large enhancement	Northern offshore and up to 1° inland	Inland propagation Before 03 LT
CJ	Small reduction	Northern inland	12–16 LT	Medium enhancement	Northern coast	Seaward propagation After 03 LT
EJ	Medium reduction	Northern inland	14–20 LT	Small enhancement	Northern coast	Seaward propagation After 03 LT

Abbreviations

CENS	Cross equatorial northerly surge
DCR	Diurnal cycle of rainfall
MC	Maritime Continent
SCS	South China Sea
WJ	Western Java
CJ	Central Java
EJ	Eastern Java
LT	Local time
MCS	Mesoscale convective system
MJO	Madden-Julian Oscillation
VIMFC	Vertical integrated moisture flux convergence
OS	Offshore
CS	Coastal sea
CL	Coastal land
MT	Mountainous area
CAPE	Convective available potential energy

Supplementary Information

The online version contains supplementary material available at https://doi.org/10.1186/s40562-023-00293-8.

Additional file 1. A comparison of (a) IMERG V06, (b) GSMaP V7, and (c) ERA5 daily rainfall anomaly [shaded; mm day^{-1}] during CENS (CENS minus climatology).

Additional file 2. Spatial distribution of composite of (a–c) surface latent heat flux [shaded; Watt m^2], (d–f) surface air temperature [shaded; K], and (g–i) relative humidity (shaded; %) during (a, d, g) nonCENS, (b, e, h) CENS, and (c, f, i) difference between CENS and nonCENS.

Additional file 3. Number of CENS and nonCENS days coinciding with MJO phases from DJF 2000/2001 to 2019/2020. MJO data are freely accessed from http://www.bom.gov.au/climate/mjo/.

Acknowledgements

We would like to express our gratitude to Prof. Junshi Ito for his helpful comment in the early stage of this work. Discussions with Prof. Guixing Chen were also valuable at the early stage of this work. MTM is grateful for the support of the Ministry of Education, Culture, Sports, Science, and Technology of Japan (MEXT) through scholarship in the International Graduate Program of Advance Science (IGPAS) program. MRA is partly supported by the Institute for Research and Community Services of Institut Teknologi Bandung (LPPM ITB) and PPMI Riset Kolaboratif ITB.

Author contributions

M.T.M. conducted data processing and analyses, generated figures, and drafted the manuscript. T.Y. provided helpful insight in the analysis, editorial aspects, and revised the manuscript. T.I. provided helpful insight to improve the analyses and revised the manuscript. M.R.A. provided technical guidance and revised the manuscript. All authors discussed the results and manuscript at all stages. All authors have read and approved the final manuscript.

Funding

None.

Availability of data and materials

The IMERG data sets provided by Goddard Earth Sciences Data and Information Services Center (GES DISC) are available at https://gpm1.gesdisc.eosdis.nasa.gov/data/GPM_L3/GPM_3IMERGHH.06/. The ERA5 pressure levels and single levels data sets provided by the Climate Data Store (CDS) Catalogue are available at https://cds.climate.copernicus.eu/cdsapp#!/dataset/reanalysis-era5-pressure-levels?tab=form and https://cds.climate.copernicus.eu/cdsapp#!/dataset/reanalysis-era5-single-levels?tab=form.

Declarations

Competing interests

The authors declare that they have no competing interests.

Received: 7 October 2022 Accepted: 9 August 2023
Published online: 29 August 2023

References

Abdillah MR, Kanno Y, Iwasaki T, Matsumoto J (2021) Cold surge pathways in East Asia and their tropical impacts. J Clim 34(1):157–170. https://doi.org/10.1175/JCLI-D-20-0552.1

Andi YIW, Rakhmat P, Rahman AA, Takahiro O, Masahiko N (2020) An assessment of IMERG rainfall products over Bali at multiple time scale. E3S Web of Conferences 153:02001

Hattori M, Mori S, Matsumoto J (2011) The cross-equatorial northerly surge over the maritime continent and its relationship to precipitation patterns. J Meteorol Soc Jpn 89A:27–47. https://doi.org/10.2151/jmsj.2011-A02

Hermawan E, Lubis SW, Harjana T, Purwaningsih A, Risyanto RA, Andarini DF, Ratri DN, Widyaningsih R (2022) Large-scale meteorological drivers of the extreme precipitation event and devastating floods of early-February 2021 in Semarang, Central Java, Indonesia. Atmosphere 13(7):1092. https://doi.org/10.3390/atmos13071092

Hersbach H, Bell B, Berrisford P, Hirahara S, Horányi A, Muñoz-Sabater J, Nicolas J, Peubey C, Radu R, Schepers D, Simmons A, Soci C, Abdalla S, Abellan X, Balsamo G, Bechtold P, Biavati G, Bidlot J, Bonavita M, Chiara G, Dahlgren P, Dee D, Diamantakis M, Dragani R, Flemming J, Forbes R, Fuentes M, Geer A, Haimberger L, Healy S, Hogan RJ, Hólm E, Janisková M, Keeley S, Laloyaux P, Lopez P, Lupu C, Radnoti G, Rosnay P, Rozum I, Vamborg F, Villaume S, Thépaut J (2020) The ERA5 global reanalysis. QJR Meteorol Soc 146(730):1999–2049. https://doi.org/10.1002/qj.3803

Hou AY, Kakar RK, Neeck S, Azarbarzin AA, Kummerow CD, Kojima M, Oki R, Nakamura K, Iguchi T (2014) The global precipitation measurement mission. Bull Amer Meteor Soc 95(5):701–722. https://doi.org/10.1175/BAMS-D-13-00164.1

Houze RA Jr, Geotis SG, Mark FD Jr, West AK (1981) Winter monsoon convection in the vicinity of North Borneo. Part I: Structure and time variation of the clouds and precipitation. Mon Weather Rev 109:1595–1614

Huffman GJ, Stocker EF, Bolvin DT, Nelkin EJ, Jackson T (2019) GPM IMERG Final Precipitation L3 Half Hourly 0.1 degree x 0.1 degree V06, Greenbelt, MD, Goddard Earth Sciences Data and Information Services Center (GES DISC), Accessed: November 2020, 10.5067/GPM/IMERG/3B-HH/06

Koseki S, Koh T-Y, Teo C-K (2013) Effects of the cold tongue in the South China Sea on the monsoon, diurnal cycle and rainfall in the Maritime Continent: climatic Effects of South China Sea Cold Tongue. QJR Meteorol Soc 139(675):1566–1582. https://doi.org/10.1002/qj.2052

Krismon A, Abdillah MR, Trilaksono NJ (2022) Modulation of diurnal cycle of rainfall over the western maritime continent associated with cold surge and the Madden–Julian oscillation. In: Yulihastin E, Abadi P, Sitompul P, Harjupa W (eds) Proceedings of the international conference on radioscience, equatorial atmospheric science and environment and humanosphere science, 2021. Springer Nature, Singapore, pp 583–592

Mori S, Jun-Ichi H, Tauhid YI, Yamanaka MD, Okamoto N, Murata F, Sakurai N, Hashiguchi H, Sribimawati T (2004) Diurnal land–sea rainfall peak migration over Sumatera Island, Indonesian maritime continent, observed by TRMM satellite and intensive Rawinsonde soundings. Mon Weather Rev 132(8):2021–2039. https://doi.org/10.1175/1520-0493(2004)132%3c2021:DLRPMO%3e2.0.CO;2

Mori S, Hamada J-I, Hattori M, Wu P-M, Katsumata M, Endo N, Ichiyanagi K, Hashiguchi H, Arbain AA, Sulistyowati R, Lestari S, Syamsudin F, Manik T, Yamanaka MD (2018) Meridional march of diurnal rainfall over Jakarta, Indonesia, observed with a C-band Doppler radar: an overview of the HARIMAU2010 campaign. Prog Earth Planet Sci 5(1):47. https://doi.org/10.1186/s40645-018-0202-9

Nuryanto DE, Pawitan H, Hidayat R, Aldrian E (2019) Characteristics of two mesoscale convective systems (MCSs) over the Greater Jakarta: case of heavy rainfall period 15–18 January 2013. Geosci Lett 6(1):1. https://doi.org/10.1186/s40562-019-0131-5

Qian J-H (2008) Why precipitation is mostly concentrated over islands in the maritime continent. J Atmos Sci 65(4):1428–1441. https://doi.org/10.1175/2007JAS2422.1

Qian J-H, Robertson AW, Moron V (2010) Interactions among ENSO, the monsoon, and diurnal cycle in rainfall variability over Java, Indonesia. J Atmosp Sci 67(11):3509–3524. https://doi.org/10.1175/2010JAS3348.1
Ramadhan R, Marzuki M, Yusnaini H, Muharsyah R, Suryanto W, Sholihun S, Vonnisa M, Battaglia A, Hashiguchi H (2022a) Capability of GPM IMERG products for extreme precipitation analysis over the Indonesian maritime continent. Remote Sensing 14(2):412. https://doi.org/10.3390/rs14020412
Ramadhan R, Yusnaini H, Marzuki M, Muharsyah R, Suryanto W, Sholihun S, Vonnisa M, Harmadi H, Ningsih AP, Battaglia A, Hashiguchi H, Tokay A (2022b) Evaluation of GPM IMERG performance using gauge data over indonesian maritime continent at different time scales. Remote Sens 14(5):1172. https://doi.org/10.3390/rs14051172
Satiadi D, Purwaningsih A, Harjupa W, Trismidianto ADF, Nauval F, Saufina E, Harjana T, Risyanto RF, Pratama R, Devianto D, Yollanda M (2023) Impacts of CENS and MJO phenomena on diurnal cycle of local convection, moisture convergence, and rainfall over land, coast, and sea areas in the western part of Java Island. Meteorol Atmos Phys 135(5):42. https://doi.org/10.1007/s00703-023-00979-w
Saufina E, Trismidianto, Risyanto, Fathrio I, Harjupa W (2021) Impact of cross equatorial northerly surge (CENS) on Jakarta heavy rainfall and its interaction with tropical cyclone (Case study: 18–25 February 2020). AIP Conference Proceedings 2366(1):050002. https://doi.org/10.1063/5.0059995
Tan J, Huffman GJ, Bolvin DT, Nelkin EJ (2019) Diurnal cycle of IMERG V06 precipitation. Geophys Res Lett 46(22):13584–13592. https://doi.org/10.1029/2019GL085395
Trilaksono NJ, Otsuka S, Yoden S (2012) A time-lagged ensemble simulation on the modulation of precipitation over West Java in January–February 2007. Mon Weather Rev 140:16
Wu P, Hara M, Fudeyasu H, Yamanaka MD, Matsumoto J, Syamsudin F, Sulistyowati R, Djajadihardja YS (2007) The impact of trans-equatorial monsoon flow on the formation of repeated torrential rains over Java Island. SOLA 3:93–96. https://doi.org/10.2151/sola.2007-024
Wu P, Hara M, Hamada J-I, Yamanaka MD, Kimura F (2009) Why a large amount of rain falls over the sea in the vicinity of western Sumatra Island during nighttime. J Appl Meteorol Climatol 48:17
Xavier P, Lim SY, Ammar Bin Abdullah MF, Bala M, Chenoli SN, Handayani AS, Marzin C, Permana D, Tangang F, Williams KD, Yik DJ (2020) Seasonal Dependence of Cold Surges and their Interaction with the Madden–Julian Oscillation over Southeast Asia. J Clim 33(6):2467–2482. https://doi.org/10.1175/JCLI-D-19-0048.1
Yamanaka MD, Ogino S-Y, Wu P-M, Jun-Ichi H, Mori S, Matsumoto J, Syamsudin F (2018) Maritime continent coastlines controlling Earth's climate. Prog Earth Planet Sci 5:21. https://doi.org/10.1186/s40645-018-0174-9
Yulihastin E, Hadi TW, Ningsih NS, Syahputra MR (2020) Early morning peaks in the diurnal cycle of precipitation over the northern coast of West Java and possible influencing factors. Ann Geophys 38(1):231–242
Yulihastin E, Hadi TW, Abdillah MR, Fauziah IR, Ningsih NS (2022) Propagation of convective systems associated with early morning precipitation and different northerly background winds over western Java. J Meteorol Soc Jpn 100(1):99–113. https://doi.org/10.2151/jmsj.2022-005

Publisher's Note